Arch. Metall. Mater. **66** (2021), 3, 683-687

DOI: 10.24425/amm.2021.136361

YEONG-WOO CHO[1,2], JAE-JIN SIM[1,2], SUNG-GUE HEO[1,3], HYUN-CHUL KIM[1,3], YONG-KWAN LEE[1,2], JONG-SOO BYEON[1,2], YONG-TAK LEE[1,2], KEE-AHN LEE[2], SEOK-JUN SEO[1*], KYOUNG-TAE PARK[1*]

EFFECTS OF ZrO_2 AND Al_2O_3 ADDITION ON THE PHYSICAL PROPERTIES OF Cu-Mo-Cr ALLOY BY LIQUID PHASE SINTERING

In this study, the effect of the addition of ZrO_2 and Al_2O_3 ceramic powders to Cu-Mo-Cr alloy was studied by examining the physical properties of the composite material. The ceramic additives were selected based on the thermodynamic stability calculation of the Cu-Mo-Cr alloys. Elemental powders, in the ratio Cu:Mo:Cr = 60:30:10 (wt.%), and approximately 0-1.2 wt.% of ZrO_2 and Al_2O_3 were mixed, and a green compact was formed by pressing the mixture under 186 MPa pressure and sintering at 1250°C for 5 h. The raw powders were evenly dispersed in the mixed powder, as observed by scanning electron microscopy. After sintering, the microstructures, densities, electrical conductivities, and hardness of the composites were evaluated. We found that the addition of ZrO_2 and Al_2O_3 increased the hardness and decreased the electrical conductivity and density of the composites.

Keywords: Al_2O_3, ZrO_2, Cu-Mo-Cr, sintering, powder metallurgy

1. Introduction

Contact materials based on copper-chromium (Cu-Cr), with a chromium content between 15 and 50 wt.%, are widely used in vacuum interrupters for medium-voltage applications [1]. Several studies on Cu-Cr alloys have investigated the effect of metastable agglomerated precipitates on the crystal structure, friction performance, and mechanical properties [2-3]. In addition to metal alloys, the dispersion of ceramic oxides in the Cu matrix improves the mechanical properties of the Cu alloys, even at high temperatures, during contact operation. However, the research on contact materials for high-voltage vacuum interrupters is insufficient [4-5].

Cr and Mo have high melting points and hence, they exhibit excellent workability, even at high temperatures. Exceptionally fine and uniform Cr-Mo solid solution structure in the Cu-matrix interface can provide highly attractive properties, such as high strength, fracture toughness, good ductility, and corrosion resistance. Moreover, Cr and Mo can be fabricated into stable alloys, forming Cu-Cr-Mo system. This is because Cr and Mo form homogeneous solid solutions with a BCC crystal structure, equal number of valence electrons, and similar chemical properties. Mixed in any ratio, Cr-Mo exists in a single phase, even at high temperatures [6-7].

Ceramic dispersion strengthening is a suitable method for improving the mechanical properties of Cu matrix composites. Various particulate ceramic materials, such as CeO_2, WC, and Al_2O_3, have been utilized to reinforce the Cu matrix, thereby significantly enhancing the mechanical properties, as reported previously [8-9]. Among the various ceramic materials, ZrO_2 and Al_2O_3, characterized by high strength, hardness, and high melting temperatures, can be suitable reinforcing materials for Cr-Mo alloys.

In this study, the physical properties of Cu-Mo-Cr composites, before and after the addition of ZrO_2 and Al_2O_3 ceramics, were analyzed based on powder metallurgy. Each Cu-Cr-Mo-X (X = ZrO_2, Al_2O_3) raw material was mixed and pressed to produce a green compact. The composites were then fabricated by the Cu liquid sintering of the Cu-Mo-Cr-X green compact. The microstructures of the composite materials and their important mechanical properties, including electrical conductivity, hardness, and density, were examined.

[1] KOREA INSTITUTE FOR RARE METALS, KOREA INSTITUTE OF INDUSTRIAL TECHNOLOGY, 7-50 SONGDO-DONG YEONSOO-GU, INCHEON 21999, KOREA
[2] INHA UNIVERSITY, DEPARTMENT OF ADVANCED MATERIALS ENGINEERING, INCHEON 22212, KOREA
[3] KOREA UNIVERSITY, DEPARTMENT OF MATERIALS SCIENCE AND ENGINEERING, SEOUL 02841, KOREA

* Corresponding authors: ktpark@kitech.re.kr; sjseo@kitech.re.kr

2. Experimental details

Cu, Mo, Cr, ZrO_2, and Al_2O_3 elemental powders (Avention co. ltd., Korea) were used in the experiments; their purities, particle sizes, and particle morphologies are summarized in Table 1. All alloy compositions are expressed in wt.%, unless stated otherwise. The composition ratio of the metal powders, Cu:Mo:Cr, was 60:30:10 (wt.%), in which a small amount of ceramic powder was added. A commercial planetary ball mill, using WC balls (diameter 10 mm, 5 mm) at a ball-to-powder weight ratio (BPR) of 5:1, was used for grinding the metal powders. The speed of the ball mill was 200 rpm for 4 h, throughout the milling. The ball-milled powder was loaded into a steel mold and pressurized at 186 MPa for 3 min to produce a 93 mm diameter green compact. This green compact was transferred into an alumina crucible, heated at a rate of 10°C/min, and subsequently maintained at a temperature of 1250°C for 5 h under Ar atmosphere. Fig. 1 illustrates the overall process sequence. The microstructure of the mixed powder and composite, after sintering, was observed via scanning electron microscopy/energy dispersive X-ray spectroscopy (SEM/EDS, JEOL, JSM-7100F). The actual density of the composites, produced by sintering, was measured by using the Archimedes' principle, and the relative density, $\rho_{relative}$, was calculated using Eq. (1) as:

$$\rho_{relative}(\%) = \frac{\rho_{actual}}{\rho_{theoretical}} \times 100 \quad (1)$$

Here, ρ_{actual} and $\rho_{theoretical}$ are the measured and theoretical densities of a sample, respectively. The electrical conductivity was analyzed by passing an eddy current across a cross-section using an electrical conductivity meter (SIGMASCOPE, SMP350). The electrical conductivity was calculated using the International Annealed Copper Standard (IACS). The hardness was measured by pressurizing the composites for 10 s with a test load of 0.1 kgf using a Vickers hardness tester (Mitutoyo, HM210A).

TABLE 1

Elemental powders used in the mechanical alloying

Elemental powder	Purity (wt.%)	Particle size (μm)	Particle morphology
Cu	99.9	d(50) : 25.9 mean : 28.2	Dendritic
Mo	99.9	d(50) : 25.2 mean : 27.2	Close to Spherical
Cr	99.9	d(50) : 16.3 mean : 19.7	Flake
ZrO_2	99.9	d(50) : 39.5 mean : 40.2	Close to spherical
Al_2O_3	99	d(50) : 98.3 mean : 99.8.	Close to spherical

3. Results and discussion

Fig. 2 shows the SEM image of the mixed raw material after ball milling. Although most powders retained their particle shapes, particles of some Cu powders changed from their initial agglomerated dendritic morphology to a plate shape. The particle size of ZrO_2 decreased from approximately 40 μm to 20 μm. In the case of Al_2O_3, some particles were not pulverized and remained 100 μm in size. As milling continued, the ZrO_2 and Al_2O_3 hard particles either deformed further or retained their shapes, and were gradually embedded into the soft Cu particles. After ball milling, most of the metals mixed and mechanically combined. However, a portion of the ceramic particles retained their shapes and were not alloyed. This indicated that sintering of the green compact, produced after pressing the mixed powder, may create voids owing to the ceramic particles that were deformed or retained their shape, resulting in the formation of pores in the composite [10-13]. The uniform distribution of additives in the Cu base, which is the main conductivity channel, degrades the electrical properties; however, it increases the hardness, thereby improving the overall physical properties. As the Cu powder exhibits low ductility and undergoes flaking during ball milling, it is possible to obtain a more uniform additive dispersion effect by evenly dispersing the additive on the flaked surface. The mixed powder was molded at a pressure of 186 MPa to produce a green compact, and then sintered as described earlier. The specimen was then polished, and the microstructure of the composite was observed.

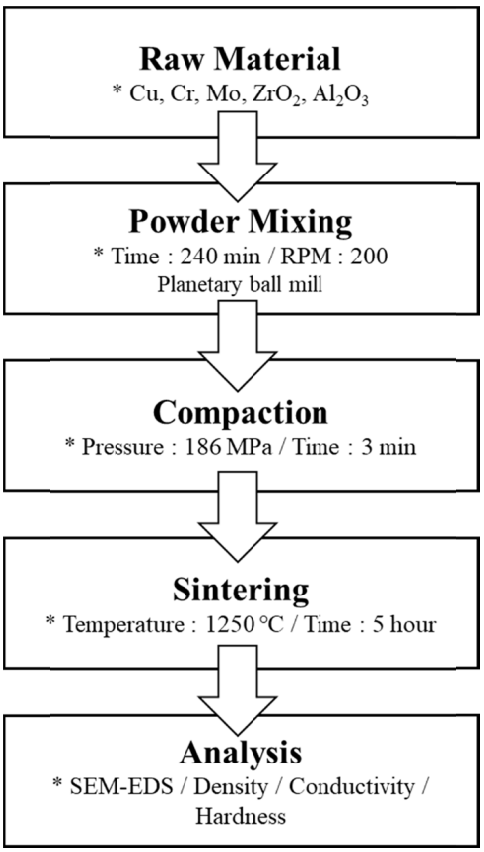

Fig. 1. Schematic flowchart of the experiment

Fig. 3 shows the cross-sectional structure of each Cu-Mo-Cr-X composite, after pressing and sintering the mixed powder. The microstructures of Cu, Mo, and Cr, before adding the ceramics, were uniformly distributed. Some Cr phases were

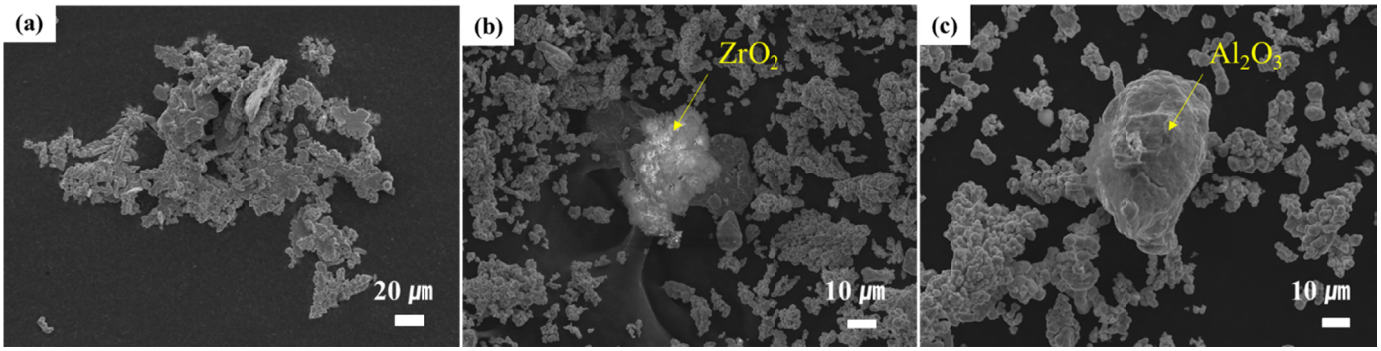

Fig. 2. SEM images of Cu-Mo-Cr-X powder mixed by ball milling. (a) Cu-Mo-Cr mixed powder, (b) Cu-Mo-Cr-ZrO_2 mixed powder, and (c) Cu-Mo-Cr-Al_2O_3 mixed powder

agglomerated separately. Despite the homogeneous solid solution (Mo, Cr), some differences were observed in the contrasts of the backscattered electron/EDS images. ZrO_2 was evenly dispersed in the microstructure. The microstructure with a ZrO_2 content of 0.8 wt.% or less exhibited a compact and crack-free structure with a uniform distribution of metal particles. Contrarily, an increase in the Al_2O_3 content did not lead to partial dispersion of the alumina particles, and consequently, the microstructure of the composite material developed cracks, indicating increased porosity of the composites [12-14]. The microstructure of the composite, comprising only metallic materials without Al_2O_3 or ZrO_2, was more uniform.

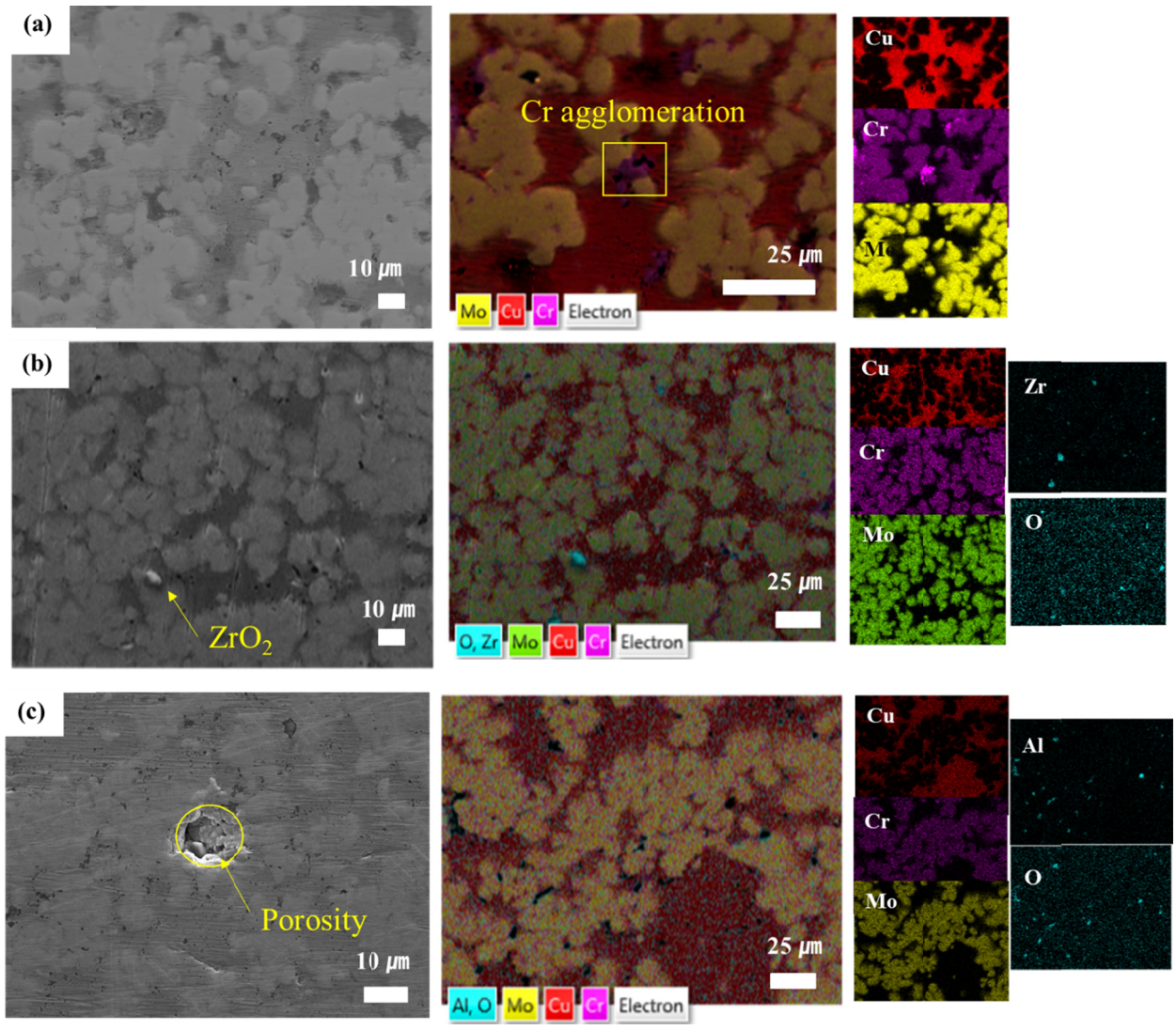

Fig. 3. SEM-EDS images of Cu-Mo-Cr-X composite after sintering. (a) Cu-Mo-Cr composite, (b) Cu-Mo-Cr-ZrO_2 (0.8 wt.%) composite, and (c) Cu-Mo-Cr-Al_2O_3 (1.2 wt.%) composite

Fig. 4 shows the physical characteristics of the Cu-Mo-Cr-X (X = ZrO_2, Al_2O_3) composite. The theoretical density of the composite material was calculated from the volume fraction (vol.%), which is expressed by Eq. (2.1), and the elemental density (g/cm^3) of each material. The theoretical density of the composite material is expressed by Eq. (2.2), in terms of the volume fraction.

$$V_{af}(\%) = \frac{\frac{W_a}{D_a}}{\frac{W_a}{D_a}+\frac{W_b}{D_b}+\frac{W_c}{D_c}+\frac{W_d}{D_d}} \quad (2.1)$$

$$\rho_{theoretical}\left(\frac{\text{g}}{\text{cm}^3}\right) = (V_a \cdot D_a)+(V_b \cdot D_b)+ \\ +(V_c \cdot D_c)+(V_d \cdot D_d), \text{ for } V_a+V_b+V_c+V_d = 1 \quad (2.2)$$

The volume fraction (W_{af}) of each raw material is the percentage of the raw material volume content in the total volume calculated from the weight fraction (W) and elemental density of the raw material powder. In the above equations, V_a ($\sim V_c$) is the volume fraction of the metal, V_d is the volume fraction of the oxide, and D is the theoretical density of each material [15]. Fig. 4(a) shows the variation of density and relative density with increasing ZrO_2 and Al_2O_3 contents. Before the addition of the ceramic, the relative density was the highest, at 90 %, and when 1.2 wt.% ZrO_2 was added, the relative density became the lowest, at 79.9 %. With the increasing ZrO_2 and Al_2O_3 contents, the density showed a decreasing trend, and when the ZrO_2 content was 1 wt.% or more, it decreased rapidly. This indicates that as the ceramic content increased, the ceramic particles did not disperse and the pores generated due to agglomeration resulted in a lower density [10,14-16].

Fig. 4(b) shows that the electrical conductivity decreased as the ZrO_2 and Al_2O_3 contents increased. Prior to the ceramic addition, the electrical conductivity was the highest, at 40.5 %IACS, and when 1.2 wt.% ZrO_2 was added, it became the lowest, at 33.1 %IACS. The theoretical electrical conductivity, modeled by the effective medium approximation (EMA) or effective medium theory (EMT), was calculated using Eq. (3). This equation can be used to successfully predict the electrical conductivities of composites in which the conductivities of the matrix and additive phases differ significantly (particularly when the conductivity of one phase is nearly zero).

$$\sigma_{eff} = \sigma_2 \cdot \left(\frac{f_2 - f_c}{1 - f_c}\right), \text{ for } f_2 \geq f_c \quad (3)$$

where σ_{eff} is the theoretical electrical conductivity of the phase, σ_2 is the electrical conductivity of the Cu-Mo-Cr product, f_2 is the volume fraction of the conducting phase (CuMoCr), and f_c is the predicted critical volume fraction of the conducting phase. The ceramic particles are assumed to be spherical single-phase particles, and the EMT predicted critical volume fraction of the conduction phase is f_c = 1/3, in 3D [17-18]. As shown, the composites, without the addition of ceramics, can achieve high electrical conductivities. Because the conductivity of the Cu region is the highest, current flows through the Cu region rather than the ceramic additives, in the sintered body. Therefore, as ZrO_2 and Al_2O_3 are distributed in the Cu matrix, they negatively affect the matrix conductivity by blocking the transfer of electrons in Cu. Furthermore, with increasing ceramic concentration, the effect of pores or cracks in the vicinity of the interface between the metal matrix and ceramic additive can be increased. The presence of these voids or cracks can also contribute to the difference between the theoretical and measured electrical conductivities [19-20].

Fig. 4(c) shows that the material hardness increases as the ZrO_2 and Al_2O_3 contents are increase. The highest hardness of 275 HV and 238 HV were obtained for 1.2 wt.% ZrO_2 and Al_2O_3 addition, respectively. The hardness of a material is a physical parameter that describes its ability to resist localized plastic deformation. The high hardness of Al_2O_3 (theoretical hardness is 1700 HV) and ZrO_2 (theoretical hardness is 1200 HV) increased the hardness of the composite material. In addition, as the contents of ZrO_2 and Al_2O_3 increased, the ZrO_2 and Al_2O_3 particles were embedded in the Cu-Mo-Cr matrix, preventing the grain boundary slip of the Cu-Mo-Cr matrix. The dispersion of particles in the Cu-Mo-Cr matrix hindered its dislocation motion due to plastic deformation. The composite material with Al_2O_3 exhibited a smaller increase in hardness than that with ZrO_2 because of the formation of cracks and pores by the large Al_2O_3 particles, which were only partially crushed [16,20-21].

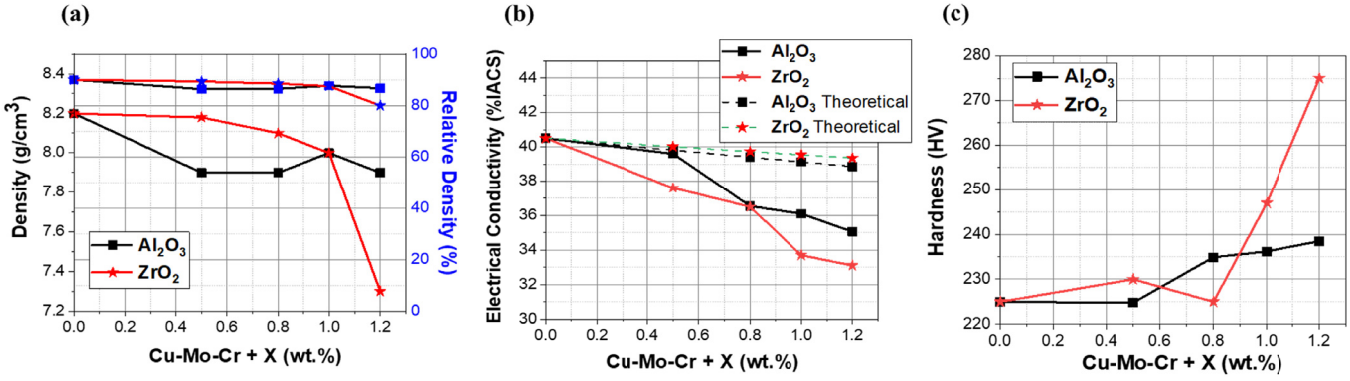

Fig. 4. Physical properties of the Cu-Mo-Cr-X (X = ZrO_2 and Al_2O_3) composite

4. Conclusion

In this study, the physical properties of the Cu-Mo-Cr-X (X = ZrO_2, Al_2O_3) composite were analyzed by SEM-EDS, density and electrical conductivity measurements, and hardness tests. The following conclusions were drawn:

1. As the Al_2O_3 content increased, the Al_2O_3 particles in the composite material were not evenly dispersed, which led to the formation of cracks. Therefore, pore formation or segregation occurred.
2. Before the addition of ZrO_2 and Al_2O_3, the material exhibited the highest relative density (90 %) and electrical conductivity (40.5 %IACS); the highest hardness (275 HV) was obtained when 1.2 wt.% of zirconia was added.
3. Considering the overall electrical properties of the electrical contact material, optimal properties were obtained when no ceramic was added. However, to improve the mechanical properties, it is necessary to introduce a small amount of ceramic material.
4. For application in high-voltage vacuum interrupters, a small amount of ceramic should be added into the electrical contact material to secure abrasion resistance without reducing its density and electrical conductivity.

Acknowledgment

This study was supported by the Korea Institute of Energy Technology Evaluation and Planning (KETEP), the Ministry of Trade, Industry & Energy (MOTIE) of the Republic of Korea (No. 20165010100870), the Korea Technology and Information Promotion Agency for SMEs (TIPA), and the Ministry of SMEs and Startups of the Republic of Korea (No. S2761733).

REFERENCES

[1] W.P. Li, R.L. Thomas, R.K. Smith, IEEE Trans. Plasma Sci. **29** (5), 744-748 (2001).

[2] X. Wei, J. Wang, Z. Yang, Z. Sun, D. Yu, X. Song, B. Ding, S. Yang, J. Alloys Compd. **509**, 7116-7120 (2011).

[3] H. Fink, D. Gentsch, M. Heimbach, IEEE Trans. Plasma Sci. **31**, 973-976 (2003).

[4] K. Maiti, M. Zinzuwadia, J. Nemade, J. Adv. Mat. Res. **585**, 250-254 (2012).

[5] C. Zhang, Z. Yang, Y. Wang, J. Mater. Process. Technol. **178**, 283-286 (2006).

[6] C. Aguilar, D. Guzman, F. Castro, V. Martínez, F. de Las Cuevas, S. Lascano, T. Muthiah, Mater. Chem. Phys. **146**, 493-502 (2014).

[7] M. Venkatraman, J.P. Neumann, Bull. Alloy Phase Diagr. **8**, 216-220 (1987).

[8] X. Yang, S. Liang, X. Wang, P. Xiao, Z. Fan, Int. J. Refract. Met. **28**, 305-311 (2010).

[9] S. Bera, I. Manna, Mater. Chem. Phys. **132**, 109-118 (2012).

[10] A. Kumar, S.K. Pradhan, K. Jayasankar, M. Debata, R.K. Sharma, A. Mandal, J. Electron. Mater. **46**, 1339-1347 (2017).

[11] D. Shen, Y. Zhu, W. Tong, An investigation on morphology and structure of Cu-Cr-Al_2O_3 powders prepared by mechanical milling, in: M. Wang, X. Zhou (Eds.), Proceedings of the 5th International Conference on Mechatronics, Materials, Chemistry and Computer Engineering, Atlantis Press (2017).

[12] C. Cui, Y. Gao, S. Wei, High Temp. Mater. Proc. **36**, 163-166 (2016). DOI: 10.1515/htmp-2015-0180

[13] S. Bera, W. Lojkowsky, I. Manna, Metall. Mater. Trans. A. **40**, 3276 (2009). DOI: 10.1007/s11661-009-0019-7

[14] J. Zygmuntowicz, A. Łukasiak, P. Piotrkiewicz, W. Kaszuwara, Compos. Theory Pract. **19**, 43-49 (2019).

[15] S.D. Salman, Z.B. Lemon, Natural Fibre Reinforced Vinyl Ester and Vinyl Polymer Composites. 249-263 (2018). https://doi.org/10.1016/B978-0-08-102160-6.00013-5

[16] M. Elmahdy, G. Abouelmagd, A.A. Elnaeem Mazen, J. Mat. Res. **21**, 1 (2018).

[17] M. Wang, N. Pan. J. Mater. Sci. Eng. R Rep. **63**, 1-30 (2008).

[18] J. Kováčik, Scripta Mater. **39**, 153-157 (1998). DOI: 10.1016/S1359-6462(98)00147-X

[19] M. Orolinova, J. Ďurišin, K. Ďurišinová, Z. Danková, M. Besterci, Kovove Mater. **53**, 409-414 (2015). DOI: 10.4149/km_2015_6_409

[20] Z.-Q. Wang, Y.-B. Zhong, X.-J. Rao, C. Wang, J. Wang, Z.-G. Zhang, W.-L. Ren, Z-M. Ren, Trans. Nonferrous Met. Soc. China **22**, 1106-1111 (2012).

[21] J. Zygmuntowicz, J. Los, B. Kurowski, P. Piotrkiewicz, W. Kaszuwara, Adv. Compos. Hybrid Mater. 1-11 (2020). DOI: https://doi.org/10.1007/s42114-020-00188-8